

Lack of Correlation for Sodium Iodide Symporter mRNA and Protein Expression and Analysis of Sodium Iodide Symporter Promoter Methylation in Benign Cold Thyroid Nodules

Susanne Neumann,¹ Katrin Schuchardt,^{1*} Andreas Reske,^{1*}
Alexander Reske,¹ Peter Emmrich,² and Ralf Paschke¹

Cold thyroid nodules (CTNs) are characterized by a reduced iodide uptake in comparison to normal thyroid tissue. The sodium iodide symporter (NIS) is the first step in thyroid hormone synthesis and mediates the active iodide transport in the thyroid cells suggesting that decreased iodide uptake could be a result of changes in NIS expression or molecular defects in the NIS gene. In contrast to previous studies, an intraindividual comparison of NIS mRNA expression in CTNs and their corresponding surrounding tissue was performed using direct detection of NIS mRNA. A significant reduction in NIS mRNA expression was detected in 86% of the 14 investigated CTNs. We hypothesized that human sodium iodide symporter (hNIS) transcriptional failure could be caused by primary molecular NIS gene defects and/or methylation of DNA in the NIS promoter. However, no mutation in the NIS cDNA nor in the NIS promoter region upstream up to -443 bp from the ATG start codon was detected. Therefore, primary molecular NIS gene defects were excluded. However, in 50% of CTNs with reduced NIS mRNA expression, the promoter region was hypermethylated. NIS mRNA expression in these hypermethylated CTNs only reached a maximum of 30% of the corresponding surrounding tissue. Hence, methylation of CpG islands in the NIS promoter could be a regulatory mechanism of NIS transcription in CTNs. Immunoblot revealed absent hNIS protein expression in the total cell membrane fraction in 45% of investigated nodules. In the majority of the remaining CTNs NIS protein expression was decreased in the nodule tissue compared to the corresponding surrounding tissue. For investigating protein expression immunohistochemistry has two advantages. First, the whole nodule area can be investigated, and second, NIS expression can be detected in areas where an immunoblot of a cell membrane fraction is negative. Interestingly, immunohistochemistry revealed higher NIS expression in 50% of CTNs compared to their corresponding surrounding tissues and NIS staining was predominantly intracellular. These data demonstrate that NIS protein expression does not reflect NIS mRNA expression. Therefore, factors that affect targeting of NIS to the plasma membrane are likely to be affected.

Introduction

COLD THYROID NODULES (CTNs) are a commonly diagnosed problem, especially in regions with iodine deficiency. The large majority of CTNs are benign, only approximately 5% of all nodules are malignant (1), however, thyroid carcinomas usually present as CTNs on a scintiscan. The molecular mechanisms that cause CTNs are largely unknown. CTNs are characterized by a diminished iodide uptake compared to normal thyroid tissue (2). A potential candidate

gene for alterations in iodide uptake is the sodium iodide symporter (NIS) (3). NIS mediates the active iodide uptake into thyroid cells, which represents the first step in the thyroid hormone synthesis (4,5). Since the discovery and cloning of NIS (6,7) tremendous progress has been made in understanding the mechanism of iodide transport and its possible disturbances (3-5,8). In addition, the availability of monoclonal and polyclonal antibodies against this integral membrane protein has permitted the functional characterization of NIS expression in several benign and malignant thyroid

¹III. Medical Department, University of Leipzig, Leipzig, Germany.

²Department of Neuropathology, University of Leipzig, Leipzig, Germany.

*These authors contributed equally to this work.

tissues. CTNs with a scintigraphically documented decreased iodide uptake suggest changes in NIS expression or a molecular defect in the NIS gene itself.

Higher than normal levels of NIS mRNA expression were observed in Graves' disease thyroid tissue and in toxic adenomas (9,10), whereas except for one study (11) a decreased NIS mRNA expression or a loss of NIS transcripts was detected in thyroid carcinomas and benign cold thyroid nodules (12–14). Methods to examine NIS mRNA expression as well as their results differ significantly. NIS mRNA in CTNs was undetectable by Northern analysis (10). The NIS mRNA transcript was also undetectable by nonquantitative reverse transcription-polymerase chain reaction (RT-PCR) in 1 of 11 cold benign follicular adenomas (12). An improved NIS mRNA quantification in CTNs was possible by real-time PCR. However, this study revealed a broad interindividual variation of NIS transcripts between different cold thyroid nodules (e.g., large interindividual variations of NIS mRNA). A reduction of NIS transcripts in CTNs compared to five pooled samples of normal thyroid tissues was observed with large interindividual variations ranging from 2-fold to 700-fold reductions (13). Unlike the previous studies, we investigated intraindividual differences of NIS mRNA expression by a direct comparison of CTNs with their corresponding surrounding tissue. Moreover, detection of NIS mRNA was performed by RNase protection assay, which is more sensitive than northern blot analysis and allows for direct quantification of NIS mRNA without the need for cDNA production.

In order to investigate the molecular mechanisms that may influence NIS mRNA expression in CTNs, the NIS cDNA and the promoter region upstream up to -443 bp from the ATG start codon were sequenced to search for mutations in the NIS gene, which may be responsible for the loss of iodide uptake. Furthermore, recent data suggest that DNA methylation may also be involved in the loss of NIS expression (15). Data on the distribution of CpG-islands in the human genome and the degree of methylation of these islands improve the knowledge about the processes of normal and pathologic gene expression (16,17). Alterations of the normal gene expression may occur if CpG-islands in promoter regions are hypermethylated. In several studies inactivation of tumor suppressor genes or DNA repair enzymes by hypermethylation of the promoter has been demonstrated (18,19). In papillary thyroid carcinomas with undetectable or low NIS mRNA expression the human sodium iodide symporter (hNIS) promoter was strongly methylated (15). Therefore, another aim of the present study was to investigate the methylation status of the hNIS promoter region in CTNs.

In contrast to reduced mRNA expression in CTNs, recent investigation of NIS protein expression using Western blotting revealed only slight differences between CTNs and normal tissues. However, a direct comparison between NIS mRNA and protein expression in these nodules was not performed (20). Surprisingly, immunohistochemical studies have shown NIS overexpression in some thyroid carcinomas (21), whereas in most studies a decreased mRNA was found (7,12,13).

We directly compared NIS mRNA expression in CTNs with the corresponding surrounding tissue in order to obtain a more precise result for NIS mRNA expression than it can be obtained with a normalized control group. In addition,

the protein expression was investigated by immunohistochemical studies, which have the advantages that nodule and surrounding tissue can be investigated simultaneously on one slide and information on NIS subcellular localization can be obtained. In all CTNs, in which sufficient nodule and surrounding tissue was available after surgery, the protein expression studies were extended to include an immunoblot analysis to allow for an intraindividual comparison of NIS mRNA and protein expression.

Subjects and Methods

CTN tissue samples

Tissue specimens of 42 scintigraphically CTNs and their surrounding normal tissue were obtained from surgery. All samples were immediately frozen in liquid nitrogen and stored at -80°C. Prerequisites for inclusion in the study were: (1) the identification of a solitary nodule by ultrasound, (2) a decreased technetium uptake by the nodule, and (3) the macroscopic and microscopic identification of the cold nodules by a pathologist. Thyrotropin (TSH) receptor antibodies were undetectable in all patients. Nodule and normal surrounding tissue were histologically classified according to World Health Organization (WHO) criteria (22). Clinical and histopathological data of all CTNs are summarized in Table 1.

The study was approved by the ethical committee of the University of Leipzig and the subjects gave informed consent.

The yield of nodule tissue obtained from surgery was very small in most cases. Therefore, not all nodules were available for all molecular studies.

RNA and DNA extraction

The total RNA was extracted using InViSorb RNA kit II (InViTek GmbH, Berlin, Germany). RNA samples were stored in DEPC-treated water at -20°C. Genomic DNA extraction was carried out using the QIAamp tissue kit (QIAGEN, Chatsworth, CA). Plasmid DNA preparation was performed using the QIAprep Plasmid Mini Kit (QIAGEN).

Clonality

The clonality of CTN tissue was evaluated using X-chromosome inactivation based on PCR amplification of the human androgen receptor locus as previously described (23). Fluorescence-labeled PCR products were examined using an ABI 373A Genetic Analyzer and the GeneScan Software supplied by the manufacturer (Applied Biosystems, Foster City, CA).

Generation of RNA transcription templates for RNase protection assay

The total RNA isolated from normal thyroid tissue was used to generate single-stranded cDNA (first-strand cDNA synthesis kit from Amersham Pharmacia Biotech, Braunschweig, Germany), followed by amplification of a 568-bp NIS cDNA fragment using the following primers; sense: GTG ATG CTA AGT GGC TTC TGG (cDNA position 936–956) and antisense: AAT CAC GAG TTT CCT GGG TG (cDNA position 1502–1483). This PCR fragment with an overlapping A-tail was cloned into the pGEM[®]-T vector

TABLE 1. HISTOPATHOLOGIC CHARACTERIZATION, CLINICAL FEATURES OF THE PATIENTS, AND CLONALITY OF SCINTIGRAPHICALLY COLD THYROID NODULES

Nodule	Follicular adenoma (FA)/ Adenomatous nodule (AN)	Nodule size (mm)	Clonality	TSH mU/mL	Age/Gender
CTN 1	AN	19	clonal	0.03 ^a	44/F
CTN 2	AN	26	n. i.	1.16	41/F
CTN 3	AN	39	clonal	normal	54/F
CTN 8	FA	55	clonal	0.03 ^b	16/F
CTN 9	FA	54	n. i.	0.83	54/F
CTN 10	FA	36	n. i.	—	32/M
CTN 11	FA	30	n. i.	0.03 ^b	33/M
CTN 12	AN	35	polyclonal	0.25	40/F
CTN 13	AN	36	clonal	—	48/F
CTN 16	AN	33	clonal	0.43	47/F
CTN 17	FA	46	clonal	0.66	31/F
CTN 18	AN	30	n. i.	—	43/F
CTN 19	AN	40	polyclonal	1.12	63/F
CTN 25	AN	32	clonal	1.50	30/F
CTN 32	AN	45	clonal	0.32	38/F
CTN 33	FA	32	n. i.	0.45	28/M
CTN 35	FA	33	clonal	1.51	16/F
CTN 39	AN	41	clonal	0.93	33/F
CTN 43	FA	45	clonal	0.59	25/F
CTN 46	FA	50	n. i.	0.25	74/F
CTN 50	AN	50	n. s.	0.39	30/M
CTN 51	AN	53	n. s.	0.73	34/M
CTN 53	AN	43	polyclonal	0.94	18/F
CTN 55	FA	31	polyclonal	0.80	28/F
CTN 56	AN	58	n. s.	0.5	71/M
CTN 57	FA	24	polyclonal	—	17/F
CTN 58	AN	100	clonal	normal	55/F
CTN 59	AN	23	n. s.	0.03 ^b	39/F
CTN 60	AN	55	clonal	0.92	32/F
CTN 61	AN	60	n. i.	0.61	48/F
CTN 65	FA	41	polyclonal	0.29	35/F
CTN 66	AN	16	polyclonal	0.61	50/F
CTN 67	AN	52	n. i.	0.44	57/F
CTN 68	AN	45	n. s.	1.01	73/M
CTN 69	AN	33	n. s.	1.00	62/M
CTN 70	AN	40	n. i.	0.24	34/F
CTN 71	AN	59	n. s.	0.54	29/M
CTN 72	AN	44	n. s.	0.13	34/F
CTN 73	AN	43	n. s.	0.52	40/F
CTN 74	AN	29	n. s.	0.35	55/F
CTN 75	FA	50	n. s.	0.40	45/F
CTN 76	AN	55	n.s.	1.46	23/F

Cold thyroid nodules were classified according to World Health Organization (WHO) guidelines (22). Clonality of nodules was evaluated using X-chromosome inactivation based on polymerase chain reaction (PCR) amplification of the human androgen receptor locus (23). Except for four patients, of whom two were treated with levothyroxine, all patients with scintigraphically cold thyroid nodules were euthyroid with TSH levels in the normal range (0.25–4.0 mU/mL).

^aTSH outside of the normal range.

^bPatients treated with levothyroxine.

CTN, cold thyroid nodule; n. i., not informative; n. s., not studied.

(Promega, Madison, WI). The resulting vector construct was digested with *SacII* and *SalI* (MBI Fermentas, Vilnius, Lithuania) in order to obtain a 160-bp fragment consisting of 130 bp of NIS cDNA and 30 bp of pGEM[®]-T sequence. The protruding termini were filled up by T₄-DNA-polymerase. The modified fragment was then cloned into the *EcoRV*-site of the pBluescript II SK-vector (Stratagene, Heidelberg, Ger-

many). To achieve a better termination of transcription this vector construct was cut at the *SpeI* sites in the pBluescript II SK-vector and the 30-bp pGEM-T-vector tail, respectively, and the resulting 130-bp NIS cDNA fragment of interest was then subcloned into the *SpeI* site of a pBluescript-II SK vector. The integrity of NIS cDNA in the pBluescript-II SK vector (NIS-pBSK) was verified by sequencing. To terminate the

in vitro transcription, this plasmid was cut with *NotI* (MBI Fermentas). To obtain the 75-bp GAPDH probe a pGEM-GAPDH plasmid (pGEM-vector containing a 548-bp human GAPDH cDNA fragment) was transcribed *in vitro* after digestion with *DdeI* (New England Biolabs, Schwalbach/Taunus, Germany).

Ribonuclease-Protection-Assay

The ribonuclease-protection assay (RPA) was performed using the RiboquantTM-Kit (Pharmingen, San Diego, CA). Transcription-templates NIS-pBSK and pGEMGAPDH were labeled with [α -³²P]-UTP by *in vitro* transcription using T7-RNA-polymerase. The [α -³²P]-UTP-labeled probes were hybridized for 12–16 hours at 56°C in solution in excess to different target RNA samples extracted from CTN tissue and the appropriate surrounding tissue. The remaining free probe and single stranded RNA was digested with RNases (RiboquantTM-Kit). The RNase-protected probes were purified by phenol/chloroform extraction and ethanol precipitation, then separated on a 6% polyacrylamide gel, and finally quantified by phosphoimaging on the Molecular Imager System GS-525 with the Multi Analyst Software (BIO-RAD, München, Germany) or autoradiography on Kodak Biomax Film (Deisenhofen, Germany). The ratio of NIS/GAPDH was subsequently calculated. The specificity of NIS probes was verified by hybridization with RNA extracted from Graves' disease and euthyroid goiter tissue as positive controls and with a yeast tRNA as a negative control. Two independent experiments were performed per sample.

Preparation of cDNA, RT-PCR, and direct sequencing of the NIS gene

To prepare cDNA from the total RNA of cold thyroid nodules and surrounding tissues, 2 μ g of RNA were added to a reaction mixture containing 5 \times first-strand buffer, 10 mM

dNTP, 10 μ M oligo dT primer, and 100 U Moloney murine leukemia virus reverse transcriptase (M-MLV RT; GIBCO BRL, Eggenstein, Germany). The RT reaction was carried out at 42°C for 60 minutes, 75°C for 10 minutes, and was terminated at 4°C. The NIS coding sequence was amplified from cDNA position 304 to 2422 in five overlapping fragments, ranging from 375 to 626 nucleotides. Oligonucleotide primers for amplification and sequencing of NIS cDNA and their appropriate annealing temperatures are listed in Table 2. The PCR reactions were performed in a MJ Research thermocycler PTC 200 (Biozym, Oldendorf, Germany). Amplification of NIS cDNA fragments was performed in a 50- μ L reaction mixture containing 0.5 μ g of cDNA as template, 10 μ M of each primer, 10 mM of each dNTP, 1 unit of Combi Pol polymerase (InViTek GmbH, Berlin, Germany), and the appropriate 10 \times incubation buffer with 1.5 mM MgCl₂. The PCR conditions were as follows: 30 to 35 cycles consisting of denaturation for 30 seconds at 94°C, primer annealing for 1 minute at temperatures depending on the primer used (Table 2), and extension for 1 minute at 72°C. For direct sequencing, PCR fragments were purified by polyethylene glycol (PEG) precipitation (13% PEG 8000, 10 mM MgCl₂) at room temperature. Purified PCR products were sequenced using BigDye terminator sequencing chemistry (Applied Biosystems). Sequencing reactions were analyzed on a Genetic Analyzer ABI 310 (Applied Biosystems). Furthermore, a part of the NIS promoter region upstream up to -443 bp before the ATG start codon was amplified and sequenced using genomic DNA from nodular and surrounding tissue of 13 monoclonal CTNs. The primer sequences are listed in Table 2. The PCR reaction and sequencing of purified PCR products were performed as described above.

Methylation-specific PCR analysis

This method uses PCR primer pairs to distinguish methylated from unmethylated DNA in bisulfite-modified target

TABLE 2. PRIMER FOR SEQUENCING OF NIS cDNA AND PART OF PROMOTER REGION

Primer	Sequence 5' \rightarrow 3'	Annealing temperature
sNIS 1	ACG CAG GGC GTC CGA GGA C	54°C
asNIS 1	GGT GCA GAT AAT TCC GGT	
sNIS 2	CGG GAC TTT GCA GTA CAT TG	58°C
asNIS 2	CAC AAA CAT GAC GAT GCC AC	
sNIS 3	GCT GGC CCT GCT CAT CAA	56°C
asNIS 3	GCA GGC CGG CAG GAA CAT TC	
sNIS 4	TCT CAC TCA TCT ACG GAT CGG	60°C
asNIS 4	TGG CGT CCA TTC CTG AGC TG	
sNIS 5	GTG GCT CTC TCA GTC AAC GCC TCT	60°C
asNIS 5	TAG GGT AGG GTA TTG TAG TCC T	
sNISPro	CTA GGT CTG GAG GCG GAG GTC G	64°C
asNISPro	GTA GTC CCA GGC TCC GAA GGT G	

The NIS coding sequence was amplified from cDNA position 304 to 2422 in five overlapping fragments as described in Subjects and Methods. The same primers were used for sequencing. The NIS promoter region upstream up to -443 bp before the ATG start codon and up to 51 bp after the start codon was amplified and sequenced with the primer pair NISPro. Primer NIS 3 and NIS 5 were published elsewhere (9,36).

s, sense primer; as, antisense primer; NIS, sodium iodide symporter.

DNA, in which bisulfite converts unmethylated cytosines to uracil, but 5-methylcytosines remain as cytosines (24). Two PCR reactions were performed for each DNA sample that detect originally methylated and unmethylated DNA, respectively. Modification of genomic DNA was performed as follows: 1 μ g DNA was denatured by NaOH for 10 minutes at 37°C, then treated with 10 mM hydroquinone and 5 M sodium bisulfite for 16 hours at 50°C. The modified DNA was purified using the Wizard DNACleanup system (Promega, Germany) according to the manufacturer's protocol followed by treatment with 0.3 N NaOH for 5 minutes at room temperature before ethanol precipitation. PCR with primers, which distinguish between methylated (M-primers) and unmethylated (NM-primers) DNA focusing on CpG-rich regions of the NIS promoter (start: -443 bp relative to the ATG start codon), was performed as described by Venkataraman et al. (15).

Methylation-specific PCR products of the promoter region, which were eluted from a polyacrylamide gel and purified by ethanol precipitation were sequenced using BigDye terminator sequencing chemistry (Applied Biosystems). Sequencing reactions were analyzed on a Genetic Analyzer ABI 310 (Applied Biosystems).

Production of a polyclonal NIS antibody

Peptide synthesis and antibody production was performed commercially by PINEDA Antibody Service, Berlin, Germany. A peptide corresponding to the C-terminal portion of the hNIS, amino acids 625-643 (SWTPCVGHG-GRDQQETNL) was generated by solid phase synthesis and subsequently purified. The peptide was coupled to the carrier molecule keyhole limpet hemocyanin (KLH). Three rabbits were preimmunized in intradermal manner and later immunized subcutaneously. For preimmunization on the first day, Freund's complete adjuvant, and for the first, second, and third boost Freund's incomplete adjuvant were used. Their sera were tested by Western blot analyses 60, 90, and 120 days after boosting.

Generation of a NIS-positive control for Western blot analyses

To test the specificity of polyclonal antibodies, we generated a positive control for Western blot analyses. A 501-bp hNIS cDNA-fragment (cDNA position 1831 to 2332) was amplified using the following primers: forward 5'ACGTG-GATGCACCCGGCTCTCCTCCCTGC TAAC 3' and reverse 5' ATCGTCTAGAGGCCCATCCTGAGGTTCCATCC 3'. In order to clone this fragment into the pcDNA 3.1 (+) Zeo vector (Invitrogen, Carlsbad, CA) primers containing a restriction site for *Xba*I and *Bam*HI at the 5' site were used.

Transfection of COS-7 cells

COS-7 cells were grown in Dulbecco's modified Eagle's medium (DMEM; Life Technologies, Inc.) supplemented with 10% fetal bovine serum (FBS), 1% glutamine and 1% penicillin/ streptomycin. At 75% confluence cells were subcultured in 12-well plates at a density of approximately 1×10^5 cells per well. The cells were transfected using the FUGENE 6 transfection reagent (ROCHE, Basel, Switzerland) according to the manufacturer's instructions with the pcDNA 3.1 plas-

mid containing the 501-bp hNIS fragment and with the pcDNA 3.1 vector alone. Forty-eight hours after transfection COS-7 cell membrane protein fractions were prepared.

Preparation of membrane protein fractions

Tissue samples and COS-7 cells were crushed in liquid nitrogen and resuspended in membrane preparation buffer (40 mM Tris/HCl, 250 mM sucrose, 0.1 mM dithiothreitol [DTT] and 0.1 mM phenylmethylsulfonyl fluoride [PMSF] at pH 7.4). The homogenates were first centrifuged at 700g for 10 minutes at 4°C. The supernatant was further centrifuged at 60000g for 45 minutes at 4°C to obtain the total postnuclear membrane fraction, which was resuspended in membrane preparation buffer. Protein concentrations were determined by measuring the absorption at 280 nm.

Western blot analysis

The membrane fractions of all tissue samples were heated at 37°C for 30 minutes in sample buffer (25) and electrophoresed (60 μ g of protein per lane) on 9% polyacrylamide gels containing 0.1% sodium dodecyl sulfate using a discontinuous buffer system described by Davis (26). Separated proteins were electroblotted onto nitrocellulose membranes (Schleicher & Schuell, Dassel, Germany) using a semi-dry blotting system (BioRad, Hercules, CA). The membranes were blocked with 5% nonfat dry milk in TBS/T (20 mM Tris/HCl, pH 7.6, 0.8% NaCl, 0.1% Tween 20) for 1 hour at room temperature and incubated overnight with the polyclonal NIS-antibody (dilution 1:3000) at 4°C in TBS/T containing 5% bovine serum albumin (BSA). After washing three times for 5 minutes with TBS/T, the membranes were incubated for 1 hour at room temperature with a peroxidase-conjugated anti-rabbit antibody (New England Biolabs, Beverly, MA) diluted 1:3000 in blocking solution. Membranes were washed four times in TBS/T, and subsequently membranes were incubated with the chemiluminescence reagent (SuperSignal West Pico, Pierce, Rockford, IL) for 5 minutes at room temperature. Immunoreactive proteins were detected with ChemImager 4000 (Alpha Innotech Corporation, San Leandro, CA) and quantified using Alpha Ease 4.0 software from Alpha Innotech Corporation. The measurements were repeated in two or three independent experiments.

Immunohistochemical analysis

Immunohistochemistry was performed on paraffin-embedded tissue blocks of 35 cold thyroid nodules. Several slides of 4- μ m sections were made from every block. One slide of each patient was stained with hematoxylin and eosin and reviewed by a pathologist for diagnosis and confirmation of the diagnosis benign thyroid nodule. 4 μ m sections were deparaffinated. Subsequently, microwave pretreatment for 15 minutes at 750 W was performed in citrate/Tris buffer (pH 9.0). Endogenous peroxidase activity was quenched by incubation in 3% of hydrogen peroxide for 20 minutes followed by two washes in TBS (50 mM TRIS, 150 mM NaCl, pH 7.6). Endogenous biotin activity was blocked for 20 minutes with DAKO Biotin Blocking System (DAKO Diagnostika GmbH, Germany). The slides were incubated for 1 hour with the monoclonal anti-NIS antibody (BrA 10-11, dilution 1:1000), which was kindly provided by BRAHMS Diagnos-

tica GmbH. The initial concentration of the antibody was 4 mg/mL. The slides were washed three times for 2 minutes in TBS. Afterwards the slides were incubated with a biotinylated second antibody and a peroxidase-labeled streptavidin. Staining was completed after a 5-minute incubation with diaminobenzidine substrate chromogen, which resulted in a brown-colored precipitate at the antigen site (DAKO LSAB2 System, peroxidase, DAKO Diagnostica GmbH). Finally, all slides were counterstained with hematoxylin and mounted. Three stained slides were evaluated per sample. Graves' disease tissue was used as a positive control. A papillary carcinoma without NIS immunoreactivity served as negative control.

Immunohistochemical evaluation

The slides were examined for specific immunostaining in the nodule and surrounding tissue and scored independently by two of the authors. Immunostained cells were scored as follows: no immunostaining, 0; degree I, less than 30% cells stained; degree II, 30%–70% cells stained; degree III, more than 70% of cells stained (Table 3).

Results

Histopathologic characterization and clonality

The histopathologic characterization, clonality of nodule tissues, and patients' characteristics (nodule size, TSH level, and age) are summarized in Table 1. For all 42 CTNs with reduced technetium uptake on scintiscan, a corresponding macroscopic lesion was identified during surgery. In 13 cases, follicular adenoma and in 29 cases, adenomatous nodule was classified according to WHO guidelines (22). In all

nodules, a strong histologic heterogeneity of nodule tissues was observed as seen in representative nodules in Figure 5. With the exception of 4 patients (3 treated with levothyroxine), all patients were euthyroid with a TSH level in the normal range. A clonal origin of cold nodular tissue was determined in 13 of 20 informative cases.

Determination of NIS mRNA expression

NIS mRNA expression in 14 CTNs and their corresponding surrounding tissues was examined by RNase protection assay (RPA). A 130-bp NIS mRNA fragment hybridized with the ³²P-labeled NIS *in vitro* RNA transcript probe was detectable in all tissue samples. A 75-bp GAPDH cDNA probe was used to normalize NIS mRNA transcripts for mRNA quantity. The NIS/GAPDH mRNA ratio was calculated after determination of the band intensity by densitometry (Fig. 1). Quantitative densitometry and normalization of NIS mRNA for GAPDH mRNA revealed a strongly reduced NIS expression in 86% of the cold thyroid nodules in comparison with the corresponding surrounding tissue (Fig. 3). The level of NIS mRNA expression was decreased by more than 65% in 10 CTNs (72% of the screened nodules). In 6 of these 10 nodules the NIS mRNA expression was lower than 10% (3%–9%) of the surrounding tissue (set at 100%). Two of the 14 nodules showed a decrease of NIS mRNA expression of 42%, and 32%, respectively, while no significant differences could be detected in 2 nodules (Fig. 3).

Low TSH levels were measured in 4 patients, of whom 3 patients were treated with levothyroxine (Table 1). However, the NIS mRNA expression in the 2 investigated nodules out of these 4 CTNs was similar to the other CTNs from patients with normal thyroid function (Fig. 3).

TABLE 3. ASSESSMENT OF NIS PROTEIN EXPRESSION BY IMMUNOHISTOCHEMISTRY

A				
<i>Assessment of NIS protein expression</i>				
	<i>Negative</i>	<i>I <30% IS</i>	<i>II 30%–70% IS</i>	<i>III >70% IS</i>
CTNs	2	10	19	4
<i>n</i> = 35	5.7%	28.6%	62.9%	2.8%
ST	4	10	9	1
<i>n</i> = 24	16.6%	41.6%	37.6%	4.2%
B				
<i>NIS protein expression in</i>				
<i>Nodule < ST</i>	<i>Nodule = ST</i>		<i>Nodule > ST</i>	
<i>n</i> = 3	<i>n</i> = 9		<i>n</i> = 12	
12.5%	37.5%		50%	

A: On 24 of 35 paraffin slides the surrounding tissues (ST) were available to allow a comparison with the cold thyroid nodule tissue (CTN). Nodule and surrounding tissues were separately scored in four different categories regarding their hNIS immunostaining (IS) intensity.

B: Comparison of NIS protein expression between nodule and surrounding tissue on those 24 slides with available STs.

NIS, sodium iodide symporter.

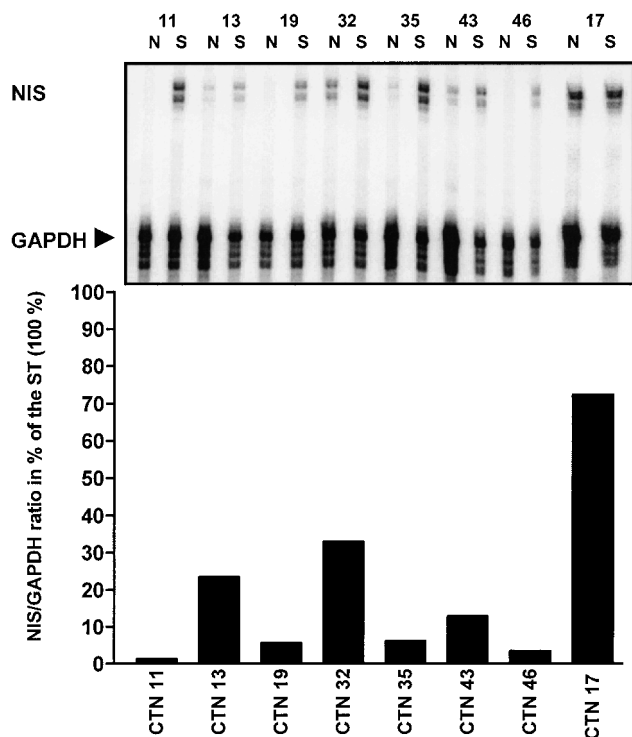


FIG. 1. Sodium iodide symporter (NIS) mRNA expression in cold thyroid nodules (CTNs) compared to their corresponding surrounding tissue (ST) analyzed by RNase protection assay (RPA). **Upper panel:** CTN tissues (N) were directly compared to the corresponding surrounding tissues (S). Fifteen micrograms of total RNA were hybridized with the ^{32}P -labeled 130-bp NIS and 75-bp GAPDH probes. After RNase digestion, the RNase protected probes were separated on a 6% polyacrylamide gel and quantified by phosphorimaging. The expected bands are indicated by black arrows. The two bands for NIS mRNA observed for all samples are specific for NIS mRNA and are most likely caused by degradation of NIS mRNA. Both NIS mRNA bands differ merely by a size of 5–7 bp. The separate determination of NIS/GAPDH ratio for these two bands yielded identical values. **Lower panel:** NIS/GAPDH mRNA ratio was calculated after the determination of the band intensity using densitometry. The NIS/GAPDH ratio of the surrounding tissue was set at 100% and the results of the CTNs were expressed as percentage of the surrounding tissues NIS/GAPDH ratio. Results from a single experiment are presented.

Direct sequencing of NIS cDNA and the promoter region –443 bp upstream of the ATG start codon

To investigate, whether reduced NIS mRNA expression in CTNs resulted from genetic alterations, the entire coding region of the NIS gene was sequenced. To increase the likelihood of finding somatic mutations only the 13 cold thyroid nodules, previously defined as monoclonal (27) (Table 1) were sequenced. No NIS mutations were found in these monoclonal CTNs. Subsequently, the search for mutations was extended to the NIS promoter region –443 bp upstream of the ATG start codon, because mutations in this region could also cause a reduced NIS transcription. Functional analyses have indicated that this promoter region contains the minimal hNIS promoter (28). This was confirmed by an-

other study, which showed that the area between nucleotides –443 to –395 is essential to confer promoter activity to the NIS gene (29). The tentative hNIS transcriptional start site is located at –375 nt upstream of the ATG site (28). However, sequencing of the NIS promoter only revealed a previously not described mutation (GGC → GGT) in 1 of 13 CTNs and the corresponding surrounding tissue 70 bp before the ATG start codon. This base pair substitution likely represents a polymorphism, because this DNA variant was also detected in 6 of 50 healthy individuals (mutation frequency > 1%) (30).

Methylation status

Methylation-specific PCR is a specific and sensitive method to determine methylation patterns of CpG islands. The hNIS promoter region, –443 bp upstream of the ATG start codon, was analyzed in 14 CTNs also investigated by RPA to investigate the hypothesis that DNA methylation in critical regulatory regions could correspond to changes in promoter activity resulting in reduced NIS mRNA expres-

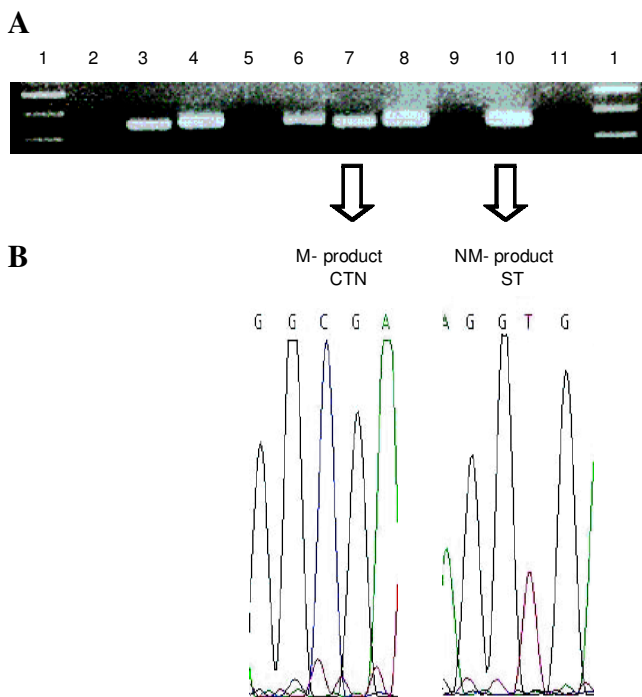


FIG. 2. Methylation analysis of the human sodium iodide symporter (NIS) promoter. **A:** Products of methylation specific polymerase chain reaction (PCR) analysis of sodium bisulfite-modified genomic DNA from nodules and surrounding tissues using a methylation specific primer pair M and a nonmethylated specific primer pair (NM) were electrophoresed on an agarose gel. Order of the samples is as follows: 1, 100-bp ladder; 2, negative control for M-primers; 3, M-product of CTN 12; 4, NM-product of CTN 12; 5, M-product of ST 12; 6, NM-product of ST 12; 7, M-product of CTN 46; 8, NM-product of CTN 46; 9, M-product of ST 46; 10, NM-product of ST 46; 11, negative control for NM-primers. Lane 4, 6, 8, and 10 contain the 151-bp NM-product. Lane 3, 5, 7 and 9 contain the 143-bp M-product. **B:** Sequence of one CpG site in the hNIS promoter of the M-PCR product of cold thyroid nodule (CTN) 46 and of the NM-PCR product of surrounding tissue (ST) 46.

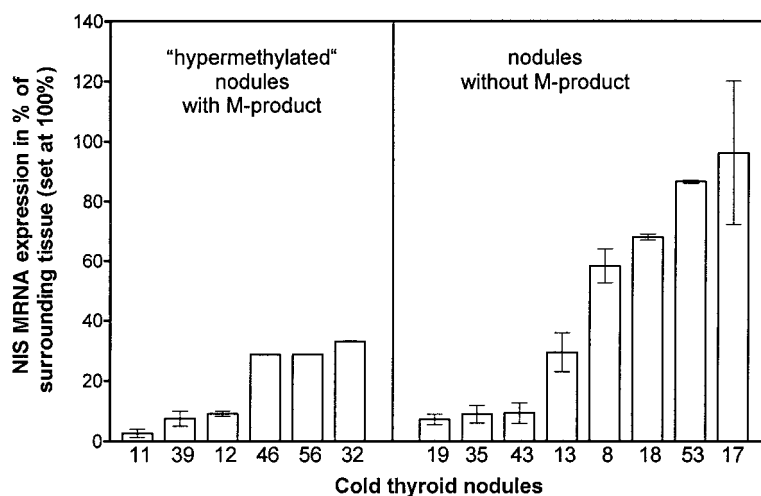


FIG. 3. Sodium iodide symporter (NIS) mRNA expression in cold thyroid nodules and correlation with the methylation status of the NIS promoter region. NIS mRNA expression in nodule and surrounding tissue was determined by RNase protection assay as described in Subjects and Methods. mRNA expression in nodule tissue is expressed in percentage of the corresponding surrounding tissue (set at 100%). Moreover analysis of DNA methylation in the NIS promoter region was performed in these nodules. In hypermethylated nodules a methylation-specific polymerase chain reaction (M-PCR) product was detectable, in other nodules no M-PCR product was detectable. The promoter region of 6 of 14 CTNs was hypermethylated. In these 6 CTNs, NIS mRNA expression reached only a maximum of 33% of mRNA expression compared to their corresponding surrounding tissues (right). In the remaining 8 CTNs, there was no apparent association of methylation with the level of NIS mRNA expression (left).

sion in these CTNs. Analysis of DNA methylation in the promoter region revealed hypermethylation in 6 out of 14 CTNs compared to their respective surrounding tissue (Fig. 2A). Sequencing of these 6 CTNs for which a PCR product could be amplified with the methylation specific (M) primer pair, revealed cytosines at the four potential CpG islands in the promoter region (Fig. 2B). Sequencing of the PCR products amplified with the nonmethylated-specific (NM) primer pair of the promoter revealed complete conversion to uracil (i.e., thymine was detected) at all CpG sites in the surrounding tissues as would be expected after bisulfite modification (Fig. 2B).

In the 6 of 14 CTNs with a hypermethylated promoter region, NIS mRNA expression only reached a maximum of 33% of mRNA expression in their corresponding surrounding tissues (Fig. 3, right side). In the remaining 8 CTNs, there was no apparent association of methylation with the level of NIS mRNA expression (Fig. 3, left side). In 3 of these 8 CTNs, NIS mRNA expression was reduced by more than 90%; furthermore, in 3 CTNs, NIS mRNA expression was reduced in the range of 70%–32% and in the other 2 CTNs, no significant difference of NIS mRNA expression was determined.

Western blot analysis

To test the specificity of the polyclonal anti-NIS antibody COS-7 cells were transfected with the pcDNA3.1 plasmid containing the 501-bp hNIS fragment and with the pcDNA3.1 vector alone. The hNIS proteins could be detected with our polyclonal anti-NIS antibody as a band with the predicted molecular weight of approximately 18 kD in COS-7 cells transfected with the pcDNA3.1 vector containing the 501-bp hNIS fragment. This band was not detected in untransfected COS-7 cells or COS-7 cells transfected with the control pcDNA3.1 vector (data not shown).

NIS protein expression in 22 CTNs and their concomitant

surrounding tissues were examined by Western blot analyses (Fig. 4). For 7 of these 22 CTNs, NIS mRNA expression was also investigated by RPA. For a further 7 nodules, which were investigated for NIS mRNA expression (in total 14 CTNs were investigated by RPA), there was insufficient tissue available for Western blot analysis. Thus, a comparison of NIS mRNA and NIS protein expression determined by immunoblot was only possible for 7 nodules.

Tissue samples showed a major band of approximately 80–90 kD, which was specific for hNIS (Fig. 4A). Several minor bands with molecular weights of approximately 60–70 kD and approximately 50 kD were also visualized in some blots. The approximately 60–70 kD bands are nonspecific, because these bands could also be visualized after competition with the peptide for the C-terminal NIS antibody. hNIS protein was undetectable in 10 of 22 CTNs. Even at higher protein concentrations (up to 150 μ g per lane), hNIS negative samples remained negative. NIS was detectable at protein concentrations of 40–60 μ g per lane in the remaining 12 CTNs. Protein expression in nodule tissue was expressed as a percentage of surrounding tissue, which was set at 100%. NIS protein expression was significantly increased in 2 CTNs ($133.3 \pm 5.4\%$ and $209.2 \pm 37.2\%$) and decreased in 10 of these 12 CTNs within the range of 16%–74%. In 7 of these 12 CTNs, NIS protein expression was decreased by more than 50% compared to the corresponding surrounding tissue (Fig. 4B). Comparison of results in a small group of 7 CTNs, which were investigated in parallel for mRNA (RPA) and protein expression by immunoblot showed that NIS protein expression did not correlate with NIS mRNA expression (data not shown).

Immunohistochemical analysis

In contrast to fresh tissue samples, of which the main part was retained for diagnostic issues, paraffin-embedded tissue was amply available from almost all CTNs. Therefore, NIS

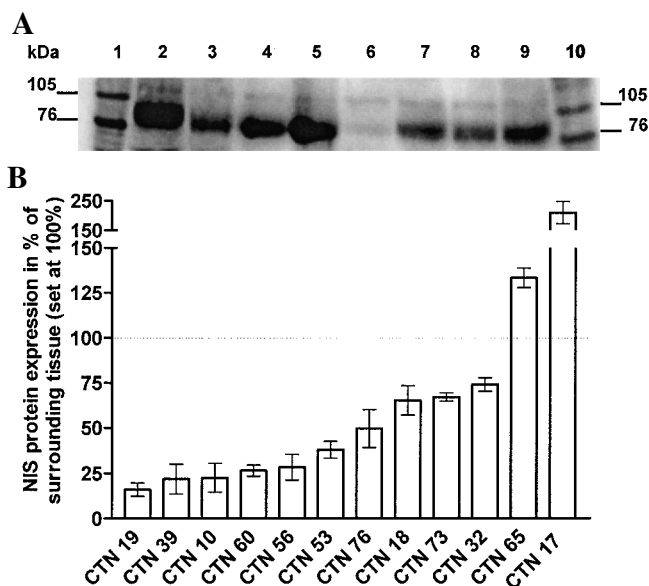


FIG. 4. Sodium iodide symporter (NIS) protein expression determined by immunoblot. **A:** NIS protein expression in cold thyroid nodules (CTNs) was directly compared to the corresponding surrounding tissue (ST). Western blotting was performed with a polyclonal anti-NIS antibody. Sixty micrograms of protein were loaded per lane. The NIS protein corresponds to an approximately 80–90 kD band. Lanes 1 and 10, protein standard; lane 2, CTN17; lane 3, ST 17; lane 4, CTN 18; lane 5, ST 18; lane 6, CTN 19; lane 7, ST 19; lane 8, CTN 32; lane 9, ST 32. **B:** NIS protein expression was detectable in 12 CTNs.

protein expression could be investigated by immunohistochemistry in 35 CTNs. A monoclonal anti-NIS antibody was used to avoid strong background noise, which we have observed with our polyclonal antibody in the cytoplasmic frac-

tion (data not shown). Because this monoclonal antibody was not suitable for immunoblot analysis, a comparison between immunoblot and immunohistochemistry with the same antibody was not possible.

NIS immunostaining was found to be heterogeneous in normal thyroid tissues as well as in CTNs. In addition, in CTNs the percentage of stained cells was highly variable and often staining was very diffuse. NIS was identified predominantly intracellularly in the majority of CTNs (Fig. 5A and 5C). In contrast, in three toxic thyroid nodules, which were examined in parallel, a predominant membrane immunoreactivity for hNIS protein was observed. However, also intracellular staining was present (Fig. 5D).

In 19 of the 35 CTNs, 30%–70% of follicular cells were positive for NIS (Table 3). However, as described above, NIS immunostaining was heterogeneous and occurred in restricted areas. For quantitative analysis of NIS expression for each nodule and surrounding tissue, the size of the areas with prominent NIS staining was quantified. In only 4 of the 35 CTNs, more than 70% of follicular cells were NIS-positive and in 10 of the 35 CTNs less than 30% stained cells were identified. Two CTNs were negative for NIS immunostaining (Table 3). In 11 CTNs there was no or not enough surrounding tissue on the paraffin-embedded tissue block available to allow a direct comparison between NIS expression in the nodule and the surrounding tissue. Surprisingly, comparison between nodule and corresponding surrounding tissue in the remaining 24 CTNs revealed that NIS protein expression was higher in nodule tissue compared to surrounding tissue in 12 of the 24 CTNs (Table 3) as shown for CTN 65 and surrounding tissue 65 (Fig. 5A and 5B). In 9 of the 24 CTNs, NIS protein expression in nodule and surrounding tissues was comparable and only for 3 of the 24 CTNs, NIS protein expression in the nodule tissues was lower than in the surrounding tissues. There was no difference between follicular adenomas and adenomatous nodules.

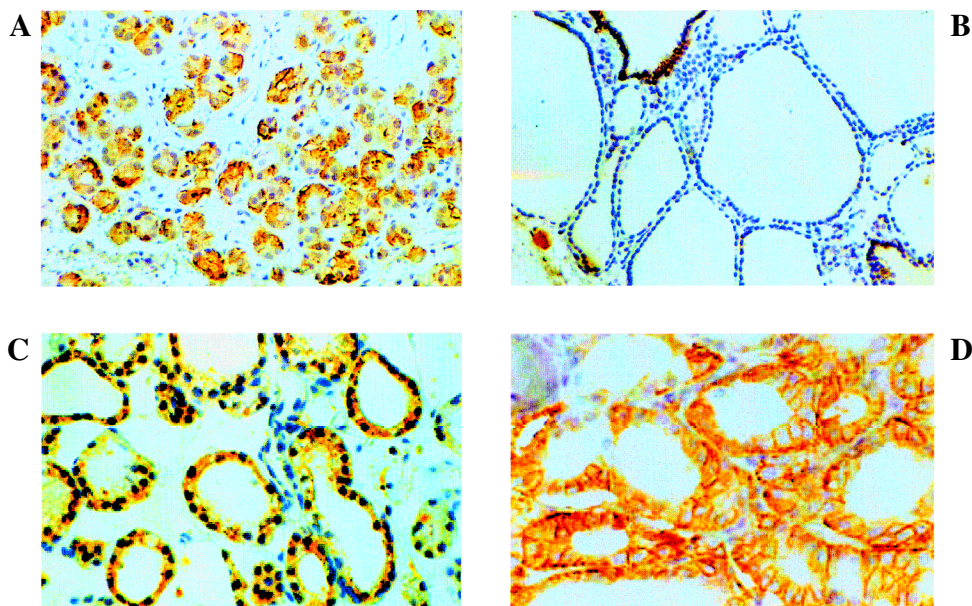


FIG. 5. Immunohistochemical analysis of NIS expression in nodule and surrounding tissue. **A:** CTN 65, nodule tissue; predominant intracytoplasmic NIS staining, only partly cell membrane immunoreactivity, **B:** CTN 65, surrounding tissue; hNIS protein immunoreactivity is low and heterogeneous, **C:** CTN 13, nodule tissue, mostly intracytoplasmic immunoreactivity, **D:** Toxic thyroid nodule; NIS cell membrane immunoreactivity is predominant.

In 17 of the 35 CTNs, a comparison between immunoblot and immunohistochemistry results was possible. However, this comparison has to be considered carefully, because we used different antibodies for both approaches. Immunohistochemical analysis clearly revealed NIS expression in nodules, which did not show NIS bands in immunoblot analysis.

Discussion

CTNs were selected by detailed histopathologic and clinical characterization (Table 1). Our study clearly demonstrates that a direct detection and quantification of NIS mRNA expression in benign CTNs is possible using RNase protection assay. Direct detection of NIS mRNA in benign CTNs as well as in nodules from euthyroid multinodular goiters was not possible in previous studies by the less sensitive Northern analysis (9,10). Moreover, intraindividual comparisons between CTNs and their concomitant surrounding tissues were performed to avoid bias by the large interindividual fluctuations described in previous studies (10,13).

We detected a significantly reduced NIS expression ranging from 3%–68% compared to the corresponding surrounding tissues in 86% of the cold thyroid nodules. This decreased NIS expression in CTNs is in line with the results of previous quantitative RT-PCR studies (10,13). However, in 20 CTNs, which were compared to 5 pooled normal tissues, a wide range of reduced NIS expression, ranging from 2-fold to 700-fold lower than in normal thyroid tissue, was detected by real-time RT-PCR (13). Our intraindividual comparison of NIS mRNA expression in CTNs tissues with their corresponding surrounding tissues revealed a much lower variation. In the 12 CTNs with a significantly decreased NIS mRNA expression, a 1.5-fold to 34-fold lower NIS expression than the surrounding tissue was determined. However, in 92% of these 12 nodules, the fold-decrease in NIS expression encompassed a much narrower range of 1.5-fold to 14-fold (Fig. 3). Hence, our study demonstrates that the exclusion of interindividual influences permits a more reliable assessment of the relative NIS mRNA expression.

The clonality of cold nodules and their surrounding tissues was characterized to identify clonal cold nodules with increased probability for mutations, because advantageous somatic mutations could induce growth stimulation and induce clonal expansion (31). To investigate whether a reduced NIS mRNA expression in clonal CTNs is caused by a primary somatic defect in the NIS gene, we sequenced the entire NIS cDNA from 13 monoclonal CTNs. Since the cloning of the human NIS, several germline mutations in this gene have been detected in patients with congenital hypothyroidism and iodide transport defects (32–37). Moreover, a mutation in the NIS gene has been identified in a patient with a huge euthyroid goiter (38). However, no somatic mutation in the entire NIS cDNA was detected in our study of monoclonal CTNs with reduced NIS mRNA expression. Moreover, in the investigated NIS promoter region (–443 bp before the ATG start codon), except for one polymorphism, no alterations were found in the 13 investigated CTNs. Although we did not sequence the entire NIS promoter, but only a minimal promoter region (28,29), primary molecular defects in the NIS gene seem to be unlikely as a major cause

for the loss of iodide uptake in cold thyroid nodules. These findings are compatible with a previous study reporting the absence of NIS gene mutations in differentiated human thyroid carcinomas, papillary and follicular carcinomas (39). Krohn et al. (27) have demonstrated that *ras* mutations are rare in solitary CTNs. In only one patient with a CTN was a N-ras mutation detected. This study also showed the absence of mutations in exon 9 and 10 of the TSH receptor in CTNs (27). Together, these results indicate that if CTNs are caused by somatic mutations, these mutations are most likely located in other perhaps yet unknown genes.

Alternatively, other factors such as alterations in the regulation of NIS transcript expression, alterations in protein synthesis or iodide organification could be involved (3). Inactivation of genes by hypermethylation of promoters can affect gene expression as drastically as mutations in the coding sequence itself (19,40). In human thyroid carcinoma cell lines, which lack hNIS mRNA, the demethylation of NIS DNA in the untranslated region within the first exon was shown to lead to a restoration of NIS transcription (15). These findings suggest a role for DNA methylation in the loss of hNIS mRNA expression in thyroid carcinomas. Moreover, they suggest a therapeutic potential that might be derived from further understanding of promoter-(de)methylation processes. In the entire group of 14 CTNs that were investigated by RPA, there was no significant correlation between NIS mRNA expression and the degree of methylation (Fig. 3). However, in 50% of cold thyroid nodules with reduced NIS mRNA expression the NIS promoter region was hypermethylated. NIS mRNA expression in these hypermethylated CTNs only reached a maximum of 30% of the corresponding surrounding tissue (Fig. 3). Moreover, in CTNs with a hypermethylated NIS promoter, there was a tendency for lower NIS mRNA expression compared to CTNs with a nonmethylated promoter (Fig. 3). Interestingly, Venkataraman et al. (15), who investigated DNA methylation in dedifferentiated thyroid tumors, also failed to define specific methylation patterns associated with transcriptional failure. Because the NIS protein is heterogeneously expressed in normal thyroid tissues (41,42), it is conceivable that DNA methylation patterns of thyroid cells are distributed in the same manner. Moreover, as previously observed by Venkataraman et al. (15) we obtained amplification with the methylated primer set as well as with the unmethylated primer set in the nodules. This suggests heterogeneous methylation in CTNs. The absence of a specific methylation pattern also indicates the importance of other epigenetic factors, which may influence NIS mRNA expression in CTNs.

It is unknown whether the reduced NIS mRNA expression correlates with NIS protein expression. Recently, in 13 CTNs investigated by Western blot analysis a similar NIS protein expression was detected in cold nodules and the non-nodular tissue (20). However, in contrast to the study of Russo et al. (20), hNIS protein was undetectable in membrane fractions by immunoblot in almost 45% of our investigated CTNs. A similar observation was also reported in the study of Ruby et al. (43), in which hNIS was undetectable in benign and malignant hypofunctioning tumors when assessed by immunoblot. In most of our nodules, NIS protein expression was decreased compared to the surrounding tissue. Because the immunoblot does not allow for determination of NIS localization within the different cellular com-

partments, we also performed immunohistochemical analyses. Some previous immunohistochemical studies reported a low (less than 20%) or undetectable NIS immunoreactivity in the majority of thyroid follicles in CTNs (41,44). In contrast to these studies (41,44) we found NIS staining of 30%–70% of the thyroid epithelial cells in two thirds of the CTNs. Moreover, a higher NIS protein expression was detected in half of all investigated nodules compared to the corresponding normal thyroid tissue when assessed by immunohistochemical analyses (Table 3). However, NIS protein expression in CTNs was mostly localized intracellularly (Fig. 5A and 5B). This result is in contrast to toxic thyroid adenomas, in which membrane immunoreactivity is predominant, but also intracellular NIS staining is visible (Fig. 5D). Our findings are consistent with a recent study, which has shown overexpressed NIS protein in 54% of benign nonfunctional thyroid nodules compared to normal surrounding tissue. NIS was mostly located inside the cytoplasm in these nodules. However, hNIS protein was absent in 46% of the nonfunctioning nodules in this study (45). In contrast in only 2 (5.7%) of our investigated nodules hNIS was not detected by immunohistochemistry. A predominant intracellular overexpression has also been reported in the majority (70%) of differentiated thyroid carcinomas (21,46). Obviously decrease in iodide uptake in most thyroid carcinomas is not caused by low NIS expression but most likely to alterations in NIS trafficking (47). Indeed, our immunohistochemical findings underscore that in CTNs a large portion of the NIS protein remains trapped in the cytosol by mechanisms, which have to be investigated in further studies as NIS targeting to the plasma membrane and retention of NIS in the plasma membrane are essential for iodide transport into the thyroid follicular cells.

NIS protein expression is upregulated by TSH *in vivo* (48), however, little is known about the mechanisms by which TSH regulates NIS expression. Recently, it was demonstrated in FRTL-5 cells that TSH regulates NIS by posttranscriptional mechanisms (49). In addition to the finding that TSH induces NIS *de novo* biosynthesis, the importance of TSH in the process of NIS targeting to or retention in the plasma membrane was demonstrated. TSH levels in almost all our patients with CTNs were in the normal range. Differences in NIS localization between CTNs and toxic thyroid nodules might indicate that the mechanisms of posttranscriptional regulation of NIS activity (5,49) are likely to be different in cold and hot thyroid nodules. However, the finding that TSH-receptor mRNA expression in toxic thyroid nodules and cold nodules are in the normal range (13) could indicate that the cyclic adenosine monophosphate (cAMP)-mediated biosynthesis of NIS cannot be the only control mechanism.

Surprisingly, we observed NIS immunostaining in CTNs in which NIS protein could not be detected by immunoblotting. One reason for this finding might be that different NIS antibodies were used in each approach. More importantly, it should be noted that membrane fractions were investigated by immunoblot, whereas examination of paraffin slides showed a predominant intracellular localization for NIS immunoreactivity. Another explanation for these differences could be the advantage of immunohistochemistry allowing the analysis of the whole nodule area, whereas tissue samples used in Western blotting only represent an average value for part of the CTN, because the larger portion

had to be used for histopathologic investigation. Moreover, the NIS distribution in thyroid tissues is heterogeneous. This could be one reason why less NIS protein was detected in some tissue areas used for immunoblot than we would have detected if we had used the whole nodule tissue. Therefore, immunohistochemical analysis seems to permit a more accurate assessment.

This study also emphasizes the necessity of intraindividual comparisons and demonstrates that NIS protein expression does not reflect NIS mRNA expression. This difference indicates that posttranscriptional factors are likely to play an important role. Moreover, reduced NIS mRNA expression does not seem to be the decisive factor in the impairment of the iodine-concentrating ability of CTNs, but posttranslational factors such as the transport of the NIS protein to the plasma membrane are likely to be disturbed in CTNs. Furthermore, alterations in other proteins interacting with or regulating NIS are conceivable in CTNs.

Acknowledgments

We would like to thank Mrs. U. Loessner for her excellent technical assistance. We wish to thank O. Dohan and N. Carrasco for helpful discussions with regard to the Western blot analysis. We thank BRAHMS Diagnostica, Berlin, for the NIS antibody used for immunohistochemical analysis. We would like to thank Dr. Schneider, Dr. Rosenkranz, Dr. Uhl, Dr. Haroske, and Dr. Thomas for access to the paraffin-embedded tissue blocks. We thank E. Ueberham (Institute of Biochemistry, Leipzig) for the GAPDH probe. This study was supported by a grant from the Deutsche Forschungsgemeinschaft (DFG/Pa423/10-1) and the Interdisciplinary Center for Clinical Research (IZKF) at the University of Leipzig (Project B20).

References

1. Castro MR, Gharib H 2000 Thyroid nodules and cancer. When to wait and watch, when to refer. *Postgrad Med* **107**:113–123.
2. Cavalieri RR, McDouglas IR 1996 In vitro isotopic tests and imaging. In: Braverman LE, Utiger R (eds) *Werner and Ingbar's The Thyroid: A Fundamental and Clinical Text*. Lippincott-Raven, Philadelphia, pp. 902–909.
3. Filetti S, Bidart JM, Arturi F, Caillou B, Russo D, Schlumberger M 1999 Sodium/iodide symporter: A key transport system in thyroid cancer cell metabolism. *Eur J Endocrinol* **141**:443–457.
4. Dohan O, De la Vieja A, Carrasco N 2000 Molecular study of the sodium-iodide symporter (NIS): A new field in thyroidology. *Trends Endocrinol Metab* **11**:99–105.
5. Riedel C, Dohan O, De la Vieja A, Ginter CS, Carrasco N 2001 Journey of the iodide transporter NIS: From its molecular identification to its clinical role in cancer. *Trends Biochem Sci* **26**:490–496.
6. Dai G, Levy O, Carrasco N 1996 Cloning and characterization of the thyroid iodide transporter. *Nature* **379**:458–460.
7. Smanik PA, Ryu K-Y, Theil KS, Mazzaferri EL, Jhiang SM 1997 Expression, exon-intron organization, and chromosome mapping of the human sodium iodide symporter. *Endocrinology* **138**:3555–3558.
8. De la Vieja A, Dohan O, Levy O, Carrasco N 2000 Molecular analysis of the sodium/iodide symporter: Impact on

- thyroid and extrathyroid pathophysiology. *Physiol Rev* **80**:1083–1105.
9. Ajjan RA, Kamaruddin NA, Crisp M, Watson PF, Ludgate M, Weetman AP 1998 Regulation and tissue distribution of the human sodium iodide symporter gene. *Clin Endocrinol (Oxf)* **49**:517–523.
 10. Joba W, Spitzweg C, Schriever K, Heufelder AE 1999 Analysis of human sodium/iodide symporter, thyroid transcription factor-1, and paired-box-protein-8 gene expression in benign thyroid diseases. *Thyroid* **9**:455–466.
 11. Saito T, Endo T, Kawaguchi A, Ikeda M, Katoh R, Kawaoi A, Muramatsu A, Onaya T 1998 Increased expression of the sodium/iodide symporter in papillary thyroid carcinomas. *J Clin Invest* **101**:1296–1300.
 12. Arturi F, Russo D, Schlumberger M, du VJ, Caillou B, Vigneri P, Wicker R, Chiefari E, Suarez HG, Filetti S 1998 Iodide symporter gene expression in human thyroid tumors. *J Clin Endocrinol Metab* **83**:2493–2496.
 13. Lazar V, Bidart JM, Caillou B, Mahe C, Lacroix L, Filetti S, Schlumberger M 1999 Expression of the Na⁺/I⁻ symporter gene in human thyroid tumors: A comparison study with other thyroid-specific genes. *J Clin Endocrinol Metab* **84**:3228–3234.
 14. Smanik PA, Liu Q, Furminger TL, Ryu K, Xing S, Mazzaferri EL, Jhiang SM 1996 Cloning of the human sodium iodide symporter. *Biochem Biophys Res Commun* **226**:339–345.
 15. Venkataraman GM, Yatin M, Marcinek R, Ain KB 1999 Restoration of iodide uptake in dedifferentiated thyroid carcinoma: Relationship to human Na⁺/I⁻ symporter gene methylation status. *J Clin Endocrinol Metab* **84**:2449–2457.
 16. Antequera F, Bird A 1993 Number of CpG islands and genes in human and mouse. *Proc Natl Acad Sci USA* **90**:11995–11999.
 17. Eng C, Herman JG, Baylin SB 2000 A bird's eye view of global methylation. *Nat Genet* **24**:101–102.
 18. Costello JF, Fruhwald MC, Smiraglia DJ, Rush LJ, Robertson GP, Gao X, Wright FA, Feramisco JD, Peltomaki P, Lang JC, Schuller DE, Yu L, Bloomfield CD, Caligiuri MA, Yates A, Nishikawa R, Su HH, Petrelli NJ, Zhang X, O'Dorisio MS, Held WA, Cavenee WK, Plass C 2000 Aberrant CpG-island methylation has non-random and tumour-type-specific patterns. *Nat Genet* **24**:132–138.
 19. Esteller M, Corn PG, Baylin SB, Herman JG 2001 A gene hypermethylation profile of human cancer. *Cancer Res* **61**:3225–3229.
 20. Russo D, Bulotta S, Bruno R, Arturi F, Giannasio P, Derwahl M, Bidart JM, Schlumberger M, Filetti S 2001 Sodium/iodide symporter (NIS) and pendrin are expressed differently in hot and cold nodules of thyroid toxic multinodular goiter. *Eur J Endocrinol* **145**:591–597.
 21. Dohan O, Baloch Z, Banrevi Z, Livolsi V, Carrasco N 2001 Predominant intracellular overexpression of the Na⁽⁺⁾/I⁽⁻⁾ symporter (NIS) in a large sampling of thyroid cancer cases. *J Clin Endocrinol Metab* **86**:2697–2700.
 22. Hedinger C, Williams ED, Sobin LH 1989 The WHO histological classification of thyroid tumors: A commentary on the second edition. *Cancer* **63**:908–911.
 23. Krohn K, Fuhrer D, Holzapfel HP, Paschke R 1998 Clonal origin of toxic thyroid nodules with constitutively activating thyrotropin receptor mutations. *J Clin Endocrinol Metab* **83**:130–134.
 24. Herman JG, Graff JR, Myohanen S, Nelkin BD, Baylin SB 1996 Methylation-specific PCR: A novel PCR assay for methylation status of CpG islands. *Proc Natl Acad Sci USA* **93**:9821–9826.
 25. Laemmli U 1970 Cleavage of structural proteins during the assembly of the head of bacteriophage T4. *Nature* **227**:680–685.
 26. Davis BJ 1964 Disc electrophoresis. II. Method and application to human serum proteins. *Ann NY Acad Sci* **121**:404–427.
 27. Krohn K, Reske A, Ackermann F, Muller A, Paschke R 2001 Ras mutations are rare in solitary cold and toxic thyroid nodules. *Clin Endocrinol (Oxf)* **55**:241–248.
 28. Ryu KY, Tong Q, Jhiang SM 1998 Promoter characterization of the human Na⁺/I⁻ symporter. *J Clin Endocrinol Metab* **83**:3247–3251.
 29. Behr M, Schmitt TL, Espinoza CR, Loos U 1998 Cloning of a functional promoter of the human sodium/iodide-symporter gene. *Biochem J* **331**:359–363.
 30. Cotton RGH, Scriver CR 1998 Proof of "disease causing" mutation. *Hum Mutat* **12**:1–3.
 31. Krohn K, Paschke R 2001 Clinical review 133: Progress in understanding the etiology of thyroid autonomy. *J Clin Endocrinol Metab* **86**:3336–3345.
 32. Fujiwara H, Tatsumi K, Miki K, Harada T, Miyai K, Takai S-I, Amino N 1997 Congenital hypothyroidism caused by a mutation in the Na⁺/I⁻ symporter. *Nature Genet* **16**:124–125.
 33. Fujiwara H, Tatsumi K, Miki K, Harada T, Okada S, Nose O, Kodama S, Amino N 1998 Recurrent T354P mutation of the Na⁺/I⁻ symporter in patients with iodide transport defect. *J Clin Endocrinol Metab* **83**:2940–2943.
 34. Kosugi S, Inoue S, Matsuda A, Jhiang SM 1998 Novel, missense and loss-of-function mutations in the sodium/iodide symporter gene causing iodide transport defect in three Japanese patients. *J Clin Endocrinol Metab* **83**:3373–3376.
 35. Pohlenz J, Medeiros-Neto G, Gross JL, Silveiro SP, Knobel M, Refetoff S 1997 Hypothyroidism in a Brazilian kindred due to iodide trapping defect caused by a homozygous mutation in the sodium/iodide symporter gene. *Biochem Biophys Res Commun* **240**:488–491.
 36. Pohlenz J, Rosenthal IM, Weiss RE, Jhiang SM, Burant C, Refetoff S 1998 Congenital hypothyroidism due to mutations in the sodium/iodide symporter. Identification of a nonsense mutation producing a downstream cryptic 3' splice site. *J Clin Invest* **101**:1028–1035.
 37. Pohlenz J, Refetoff S 1999 Mutations in the sodium/iodide symporter (NIS) gene as a cause for iodide transport defects and congenital hypothyroidism. *Biochimie* **81**:469–476.
 38. Matsuda A, Kosugi S 1997 A homozygous missense mutation of the sodium/iodide symporter gene causing iodide transport defect. *J Clin Endocrinol Metab* **82**:3966–3971.
 39. Russo D, Manole D, Arturi F, Suarez HG, Schlumberger M, Filetti S, Derwahl M 2001 Absence of sodium/iodide symporter gene mutations in differentiated human thyroid carcinomas. *Thyroid* **11**:37–39.
 40. Jaffrain-Rea ML, Ferretti E, Toniato E, Cannita K, Santoro A, Di Stefano D, Ricevuto E, Maroder M, Tamburrano G, Cantore G, Gulino A, Martinotti S 1999 p16 (INK4a, MTS-1) gene polymorphism and methylation status in human pituitary tumours. *Clin Endocrinol (Oxf)* **51**:317–325.
 41. Caillou B, Troalen F, Baudin E, Talbot M, Filetti S, Schlumberger M, Bidart JM 1998 Na⁺/I⁻ symporter distribution in human thyroid tissues: An immunohistochemical study. *J Clin Endocrinol Metab* **83**:4102–4106.
 42. Jhiang SM, Cho JY, Ryu KY, DeYoung BR, Smanik PA, McCaughy VR, Fischer AH, Mazzaferri EL 1998 An immuno-

- histochemical study of Na⁺/I⁻ symporter in human thyroid tissues and salivary gland tissues. *Endocrinology* **139**:4416–4419.
43. Ruby N, Berger F, Franc B, Perrin A, Borson-Chazot F, Rousset B 2001 Differential expression of the human Na⁺/I⁻ symporter (hNIS) and human Pendrin (hPDS) in normal tissue and tumors of the thyroid gland. Evidence that hPDS expression is not or only marginally regulated by TSH [abstract]. *J Endocrinol Invest* **24**:108.
44. Mian C, Lacroix L, Alzieu L, Nocera M, Talbot M, Bidart JM, Schlumberger M, Caillou B 2001 Sodium iodide symporter and pendrin expression in human thyroid tissues. *Thyroid* **11**:825–830.
45. Tonacchera M, Viacava P, Agretti P, De Marco G, Perri A, Di Cosmo K, De Servi M, Miccoli P, Lippi F, Naccarato AG, Pinchera A, Chiovato L, Vitti P 2003 Benign nonfunctioning thyroid adenomas are characterized by a defective targeting to cell membrane or a reduced expression of the sodium iodide symporter protein. *J Clin Endocrinol Metab* **87**:352–357.
46. Wapnir IL, Van De Rijn M, Nowels K, Amenta PS, Walton K, Montgomery K, Greco RS, Dohan O, Carrasco N 2003 Immunohistochemical profile of the sodium/iodide symporter in thyroid, breast and other carcinomas using high density tissue microarrays and conventional sections. *J Clin Endocrinol Metab* **88**:1880–1888.
47. Dohan O, De la Vieja A, Paroder V, Riedel C, Artani M, Reed M, Ginter C, Carrasco N 2003 The sodium/iodide symporter (NIS): Characterization, regulation, and medical significance. *Endocr Rev* **24**:48–77.
48. Levy O, Dai G, Riedel C, Ginter CS, Paul EM, Lebowitz AN, Carrasco N 1997 Characterization of the thyroid Na⁺/I⁻ symporter with an anti-COOH terminus antibody. *Proc Natl Acad Sci USA* **94**:5568–5573.
49. Riedel C, Levy O, Carrasco N 2001 Post-transcriptional regulation of the sodium/iodide symporter by thyrotropin. *J Biol Chem* **276**:21458–21463.

Address reprint requests to:
Ralf Paschke, M.D.
III. Medical Department
University of Leipzig
Ph.-Rosenthal-Str. 27
04103 Leipzig
Germany

E-mail: pasr@medizin.uni-leipzig.de